Light induced aggregation of cationic 1,4,5,8-Naphthalediimide bolaamphiphiles

Rafael G. Antoneli[a], Thaisa B. F. de Moraes[b,d], Helena C. Junqueira[c], Luca M. Sihn[c], Rafael Candido[a], Henrique E. Toma[c], Bruno Pedras[f], Christophe Bucher[d], Jonathan W. Steed[e], Gregóire J.-F. Demets[b], Eduardo R. Triboni[a*]

Affiliation

[a] Laboratório Nanotecnologia e Engenharia de Processos- NEP, Universidade de São Paulo, Lorena SP, Estrada Municipal do Campinho, s/nº CEP 12.602-810, Lorena, SP, Brasil. *corresponding author: tribonier@usp.br.

[b] Departamento de Química, FFCLRP, Universidade de São Paulo, Av. Bandeirantes 3900, Ribeirão Preto SP, CEP 14040-901, Brasil.

[c] Departamento de Boquímica, Instituto de Química, Universidade de São Paulo, Butantã, São Paulo - SP, CEP 05508-000, Brasil.

[d] École Normale Supérieure de Lyon, CNRS, Laboratoire de Chimie UMR 5182, 46 allée d'Italie, 69342 Lyon, France.

[e] Department of Chemistry, Durham University, South Road, Durham DH1 3LE, UK.

[f] iBB-Institute for Bioengineering and Biosciences, Instituto Superior Técnico and Associate Laboratory i4HB - Institute for Health and Bioeconomy at Instituto Superior Técnico, Universidade de Lisboa, 1049-001 Lisboa, Portugal

[g] Polytechnic Institute of Portalegre, 7300-110 Portalegre, Portugal

Abstract

Bola amphiphiles from naphthalenediimide (**NDI-bas**) with quaternary ammonium groups **(DC4**, **DaP**, and **DaO)** display association in solution, as well as, surprisingly, visible light promoted photochromism in concentrated solutions of water, acetonitrile and THF. The photochromism is correlated with an aggregation process that leads to a significant modification of the electronic transitions, resulting in an unusual absorption band distribution that points out to a type of H-aggregation in transverse. This assembly can be reversibly broken up by heating at 70 °C and adding bulk salt ($NaBF_4$). By ^{1}H-NMR spectroscopic analysis of the irradiation/heating cycle the assembly/disassembly process can be followed by the changes in peak width and intensity. These photoinduced aggregates can sensitize dissolved O_2 to give singlet oxygen, a surprising observation when it comes to sensitization efficiency for dyes where aggregation usually decreases the sensitization yield. Laser-induced luminescence measurements corroborate the existence of triplet states as phosphorescence was detected, being particularly intense in concentrated THF solutions.

1 Introduction

1,4,5,8-naphtalenediimides (**NDI**) are valuable building blocks to prepare molecular amphiphiles owing to their flat extended π-systems, photo- and thermal-stability, high electric quadrupole moment, electron affinity (a redox-active center), and easy synthesis [1-3]. Such appealing characteristics have allowed the build-up of colloidal structures as well as underpinning chemically or physically stimulated materials. **NDI** amphiphiles may be categorized as being bola, gemini, twin and zwitter. They have been designed in order to obtain nano and meso-scale functional assemblies, held mainly by π,π-interactions, H-bonding, electrostatic and charge-transfer (**CT**) interactions, often involving significant solvophobic contributions [4-6]. The shape and aggregation of **NDI**-amphiphiles in solution is intimately related to the substituent attached to the imide nitrogen or aromatic core, as well as to the solvent polarity, ionic strength, pH, and temperature. **NDI**s (as electron acceptors, **A**) display a remarkable ability to assemble with electron-rich aromatic moieties (electron donors, **D**) such as pyrene and naphthol derivatives, giving rise to donor-acceptor (**D**-**A**) arrays with different conformations and intermolecular mobilities [2,5]. Moreover, they are also very useful in the study of anion-π interactions [7-9]. **NDI** amphiphiles perform their through-space electronic events through photo-induced electron transfer (**PET**), energy transfer (**ET**), raising of **CT** transition bands, and by the formation of **NDI** reduced species (radical anions, $\mathbf{NDI}^{\bullet-}$; and dianion, $\mathbf{NDI}^{2-}$). In this light, symmetric and asymmetric alignments of acid carboxylic substituted **NDI**-amphiphiles have led to catenanes, cages and complexes structures driven by carboxylic acid hydrogen bonding and pronounced **NDI**-**NDI** π-stacking that are usually identified by absorbance shifts and by the occurrence of broad absorption bands at longer wavelengths [10,11]. The role of amide-substituted imides on the shape and mobility of vesicles has been evaluated when mixing NDI bola-amphiphiles (**NDI-ba**) and

pyrene (**py**) then monitoring the appearance of a **NDI/py CT** band centered at 565 nm [12]. Pyridyl-substituted **NDI-ba** assemblies undergo **PET** from pyridyl nitrogen to the **NDI** core forming $\mathbf{NDI}^{\bullet-}$ moieties [2]. In our previous study, semiconducting films of a positively charged **NDI-ba** enabled electrochemical photoreduction of oxygen [13]. Overall, their optical and electrical properties are very sensitive to the supramolecular organization giving rise to the nano and *meso* scale structure, prompting structure-property correlations. Generally high concentrations of the **NDI**-amphiphile are required to build these supramolecular systems, and gels are often obtained (> 1%, weight/volume ~ $>10^{-3}$ M).

Herein, the aggregation-dependent photophysical properties of bola-amphiphilic ammonium functionalized **NDI-bas** derivatives (**DC4**, **DaP** and **DaO**, Fig. 1) were evaluated in concentrated solutions with and without light exposure (λ = 365 nm, 100 W lamp) to study photo-induced aggregation. Our group has identified unique photophysical and photochemical properties when dealing with thin films or gels comprised of **NDI-bas** moieties [13, 14]. However, we opted to investigate the influence of charged N-imide groups on the assembly of **NDI-bas**, and how they behave in terms of their photophysical properties, expecting that the ammonium group might act as an electrostatic repulsive center during the association in high concentrated medium. Ammonium groups bonded to alkyl chains or carboxy-functionalized alkyl chains were chosen to ensure solubilization in different solvents and assess the possible role of the H-bonding group. UV-vis and steady state fluorescence measurements were carried out in three solvents THF, MeCN and H_2O at varying concentrations of the **NDI-bas**, as well as after illuminating the solutions for different periods (λ = 365 nm, 100 W). Without illumination all **NDI-bas** behaved as typical **NDI**s in both dilute and concentrated media. Surprisingly, however, exposure of concentrated solutions to visible light resulted in completely different spectra showing the appearance of unusual

absorption and emission bands, resulting in colored solutions, as well as pointing to a reversible interconverting system between monomers and aggregates driven by different physical stimuli. In terms of photochemical properties, the aggregates generated more singlet oxygen than single monomers, the opposite of what is usually found for most sensitizer dyes.

2 Experimental

2.1 Reagents and Materials

Naphthalene 1,4,5,8-tetracarboxylic dianhydride was purchased from TCI Chemicals. N,N´-dimethyl ethylenediamine, 2-ethanolamine, and 1-bromobutane, 3-bromopropanoic acid, 8-bromopropanoic acid purchased from Aldrich and used without further purification. Other materials and solvents were analytical grade, and water was purified via a Milli-Q system.

2.2 Characterization

The UV-VIS absorption spectra were recorded on a Shimadzu UV-1900 Spectrophotometer. Fluorescence emission spectra were recorded on a Horiba Fluoromax-4 spectrofluorometer. All photophysical measurements were carried out in a 0.5 cm optical path quartz cuvette in the frontal face mode to mitigate any possible inner filter effect. A laboratory version of the TCMPC-1270-LED (SHB Analytics GmbH, Berlin, Germany) was used for direct detection of the singlet oxygen phosphorescence kinetics. A 400 nm LED was used for excitation. Samples of equal concentration were compared. Infrared spectra were collected on a FT-IR Frontier™ MIR, directly from NDIs powders in ATR mode or KBr pellets in the range from 4000 to 500 cm^{-1}. ^{1}H-NMR spectra were recorded on a Bruker AC - 300/500 (D_2O and DMSO-$_{d6}$

solvents). Elemental Analysis CHN were done on a Perkin Elmer 2400 series ii Analyzer. To run UV and fluorescence measurements aliquots from 2.0×10^{-3} M and 2.0×10^{-2} M stock solutions, depending on the final concentration, were transferred into cuvettes to reach the desired concentration. N_2 laser (PTI model 2000, *ca*. 600 ps FWHM, ~1.0 mJ per pulse), was used in laser-induced luminescence experiments. In this case the excitation wavelength was 337 nm. The light arising from the irradiation of the samples by the laser pulse was collected by a collimating beam probe coupled to an optical fiber (fused silica) and detected by a gated intensified charge coupled device Andor ICCD, model i-Star 720 (Andor Technology Limited, Belfast, UK). The ICCD was coupled to a fixed compact imaging spectrograph (Andor, model Shamrock 163). The system can be used either by capturing all light emitted by the sample or in a time-resolved mode. The ICCD has high speed gating electronics (about 2.3 ns) and intensifier and covers at least the 250–900 nm wavelength range. Time-resolved emission spectra are available in a time range from nanoseconds to seconds. With this set-up, both fluorescence and phosphorescence spectra were easily available by the use of the variable time gate width and start delay facilities of the ICCD.

2.3 Preparation of the NDI amphiphiles

Synthesis of N,N'-(N,N-dimethylethylene)-1,4,5,8-naphthalenediimide, **1**: 1,4,5,8-naphthalic dianhydride (2 mmol, 536 mg) reacted with 5 fold excess *N,N*-dimethylethylenediamine in 40 mL ethanol under reflux for 2 h. The crude orange product was filtered, washed with water, and dried at 70 ^{o}C in an oven. Recrystallization from ethanol gave a final yield: 733 mg, 1.8 mmol, 80 %.

Alkylation: a general procedure was followed to prepare *N,N'*-(*N,N*-dimethyl ethylene-*N´*-propanoic-1,4,5,8-naphthalenediimide, **DaP**; *N,N'*-(*N,N*-dimethylethylene-*N´*-octanoic)-1,4,5,8-di-naphthalenediimide, **DaO**; and *N,N'*-(*N,N*-dimethylethylene-*N´*-butyl)-1,4,5,8-

naphthalenediimide, **DC4**, Fig.1: compound **1** (200 mg, 0.45 mmol) reacted with 3-fold molar excess of the alkylating agent (3-bromopropanoic acid, 8-bromooctanoic acid and 1-bromobutane) in acetonitrile under reflux for 8 h. All compounds formed as precipitates after solvent reduction and addition of diethyl ether solvent (30 mL). Precipitates were filtered out and washed with cold ethanol and put to dry in an oven at 70 ºC. Yields = **DaP** 268 mg, 75 %; **DaO** 320.6 mg, 83 %; **DC4** 240 mg, 70 %. Characterization data are shown in the supporting information, *SI-1*.

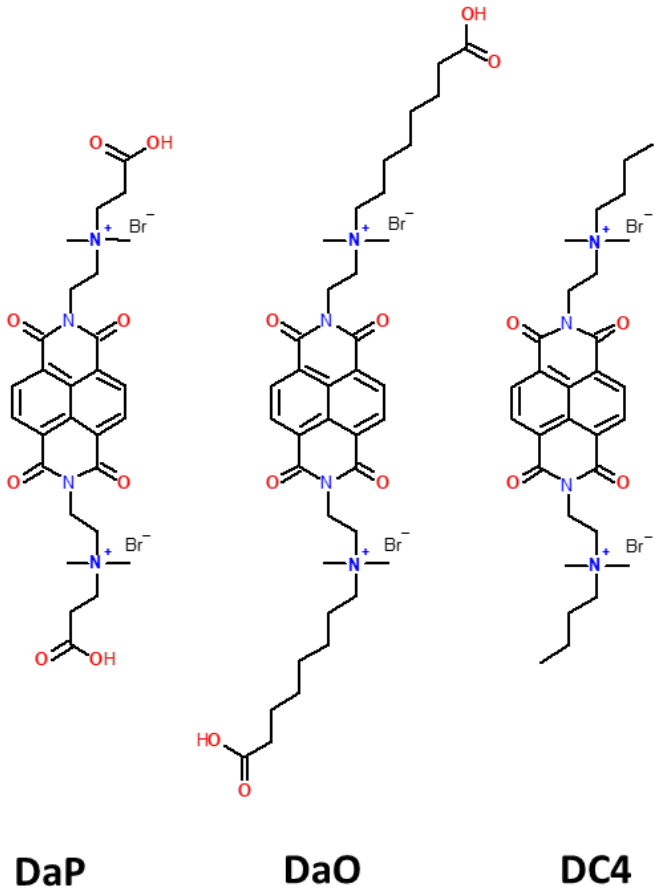

Figure 1. Substituted **NDI-ba** ammonium compounds **DaP**, **DaO** and **DC4**.

3 Results and Discussion

3.1 UV-vis and Fluorescence

The **NDI-bas** (π-π*) S0 → S1 absorbance bands showed typical NDI vibronic coupling *v* → *v´:* 0-0 ~385 nm, 0-1 ~365 nm, 0-2 ~340 nm, and 0-3 ~ 325 nm) that may reverse (0-0 to 0-1) intensity as concentration increases, Fig. 2 (supporting information, *SI-2*). This reversal has been attributed to the aggregation which changes the Franck-Condon factors [15,16]. Absorption spectra displayed hypsochromic shifts for the S0 → S1 transition when going from the more polar protic solvent (H_2O) to less polar aprotic solvent like MeCN, which is expected for π−π* electronic transitions [15]. The Fluorescence spectra of the **NDI-ba** compounds, however, exhibited quite distinct behavior depending on the solvent, Fig. 2 (supporting information, *SI-2*). Increasing **NDI-ba** concentration in H_2O and MeCN enhances emission intensities until a maximum value is reached, before diminishing at higher concentrations implying aggregation-induced quenching. Self-absorption is responsible for the disappearance of the upper energy band at λ = ~ 395 nm. On the contrary, in THF, all the **NDI-ba** compounds showed almost structureless bands, with intensity directly proportional to concentration, without any aggregate emission. Excitation spectra for **DaO** as representative model for all three compounds were recorded in H_2O and THF, Fig. 3a-b.

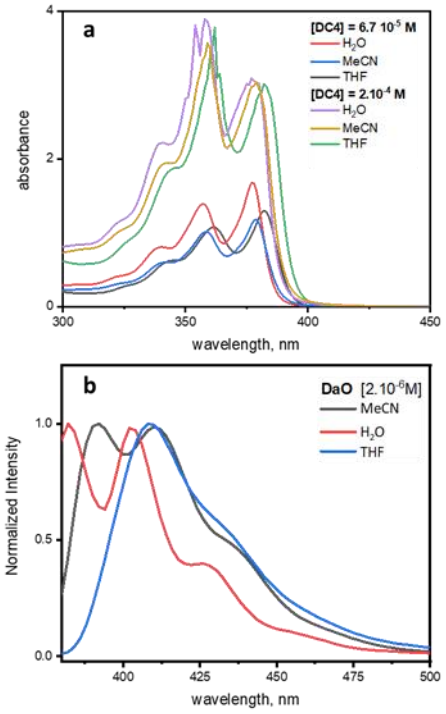

Figure 2. (a) **DaO** UV-vis spectra (6.75×10^{-5}M and 2.0×10^{-4}M); (b) **DaO** emission spectra (excitation = 365 nm). Spectra run in water, MeCN and THF.

The excitation spectrum, in H_2O, matches the UV-vis absorption spectrum at low concentration, however in a concentrated solution the S0 → S1 transition is redshifted (~ 10 nm) along with the appearance of shorter wavelength bands between 230 and 330 nm, Fig. 3. Additionally, the high energy peak maximum blueshifted from 234 to 216 nm. Unlike in H_2O, in THF, the excitation spectrum does not match the absorption spectrum showing structureless bands instead of structured ones, in addition to very different absorption patterns at low or high concentration. At high concentration, bands are centered at 326 nm and 258 nm very close to those observed in H_2O. **DaP** and **DC4** exhibited similar spectral patterns to **DaO**. These data seem to indicate an aggregation process for all these **NDI-bas** at high concentration, which modifies the transition dipoles forming

new set of bands. The straightforward relation between concentration and emission in THF points out to aggregation-induced emission phenomena [17], which will be addressed in further studies.

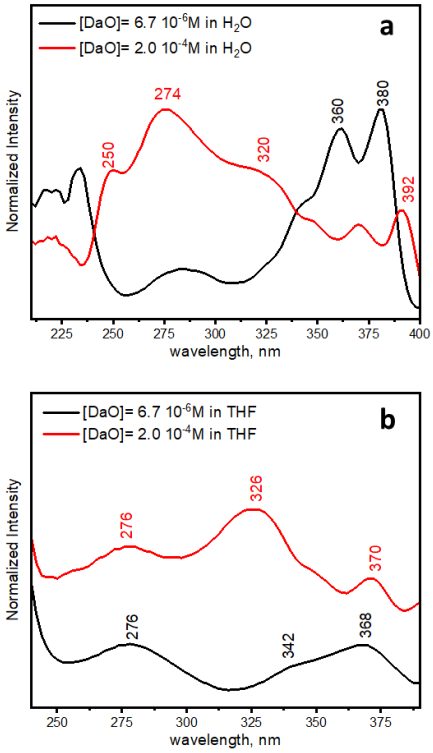

Figure 3. (a) Excitation spectra ($\lambda_{emission}$ = 415 nm) for 6.7×10^{-6} M and 2.0×10^{-4} M **DaO** in THF, and (b) in water; measurements recorded in a frontal face geometry.

3.2 Photochromism

During fluorescence measurements, the excitation beam was able to stain concentrated solutions of **NDI-bas** (> 10^{-4} M) leaving a red coloured region in the light path (*supporting information, SI-3*). To understand this photochromic property, we irradiated **DaP**, **DaO** and **DC4** solutions at different concentrations inside of a light box (power lamp 100 Watts, λ = 365 nm) for 20 min in THF, MeCN and H_2O, and we measured their UV-vis and fluorescence spectra. Experiments were carried out in the millimolar concentration range.

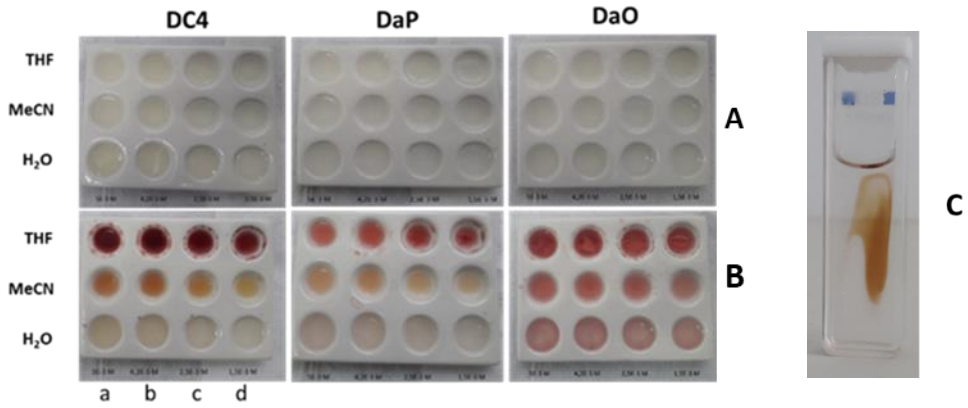

Figure 5. (A) - white translucent wells containing **NDI-ba** molecules before exposure to light, in water, MeCN and THF; (B) after 20 min illumination (power lamp 100 Watts, λ = 365 nm); a = 5.0×10^{-3} M; b = 4.2×10^{-3} M; c = 2.5×10^{-3} M; d = 1.5 10^{-3} M; (C) sensitized cuvette showing the colour change arising from irradiation inside the fluorimeter holder (in acetonitrile).

Colorless **NDI-ba** solutions turned coloured with different tones and intensities. The phenomenon was stronger in THF yielding reddish solutions. H_2O and MeCN led to weaker yellowish or reddish colours. Below 10^{-4} molar concentration there was practically no visible colour change, and among the **NDI-ba** structures, **DaO** is more susceptible to colour change at all concentrations. Despite the likelihood influence of the quaternary ammonium functional group,

photochromism depends mostly on the concentration of the amphiphiles and the solvent. Fig. 6 shows absorption and fluorescence spectra of **DaO** before and after light exposure in THF. This process is reversible with increasing temperature.

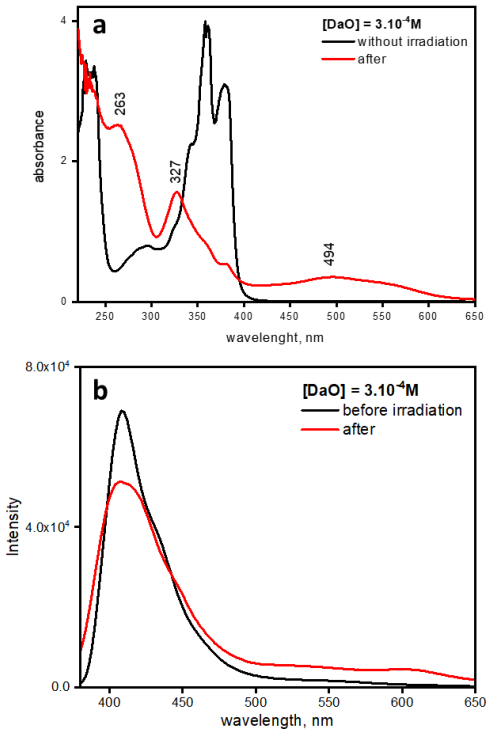

Figure 6. (a) **DaO** UV-vis and (b) fluorescence spectra in THF before and upon light exposure (λ_{exc} =365 nm).

The UV-vis spectra, for all of the **NDI-ba** compounds (*supporting information, SI-3*), display a new set of electronic transitions involving increased intensity of shorter wavelength bands (λ_{max} = 260 nm) and a spike band centered at λ = 327 nm that fits one of the vibronic modes of the S0 → S1 transition, which decreases markedly in extinction coefficient and loses band structure over time and, finally, longer wavelength broad bands rise in the region between 400 to 600 nm with λ_{max} = 490 nm. Such an absorption pattern resembles that of the excitation spectrum

(Fig. 3), and it is uncommon for NDI assemblies that often present redshifted CT-bands and reversion of the vibronic sequence [1-5, 14-16, 18]. The emission spectra, on the other hand, exhibit a small attenuation of the original peak at λ = 410 nm together with an increase in intensity of a larger band between 500 and 700 nm, which is correlated with the absorption band with a maximum at ~ 490 nm in the excitation spectrum (supporting information, *SI-3*). Hence, we postulate an absorption-emission channel that resembles the kind reported for NDI based polysilsesquioxane and organogels in which close packing among NDI units generate an emissive CT electronic state [14,19]. Combined donor-acceptor systems, for instance, electron rich aromatic rings and NDI derivatives [5], behave similarly.

Fig. 7 shows spectral evolution of the **DaO** sample with illumination time. The spectra reveal a rapidly interconverting system where continuous decrease of the intensity of the S0-S1 absorption band is linearly related to the increase in intensity of the band at 267 nm, resulting in an isosbestic point at λ = 327 nm. In addition, shorter (at 261 nm) and longer (at 490 nm) electronic bands reach a maximum to then going forward to another configuration followed by fading S0-S1 vibronic levels, as well as by concomitant redshift and decrease of the longer wavelength band.

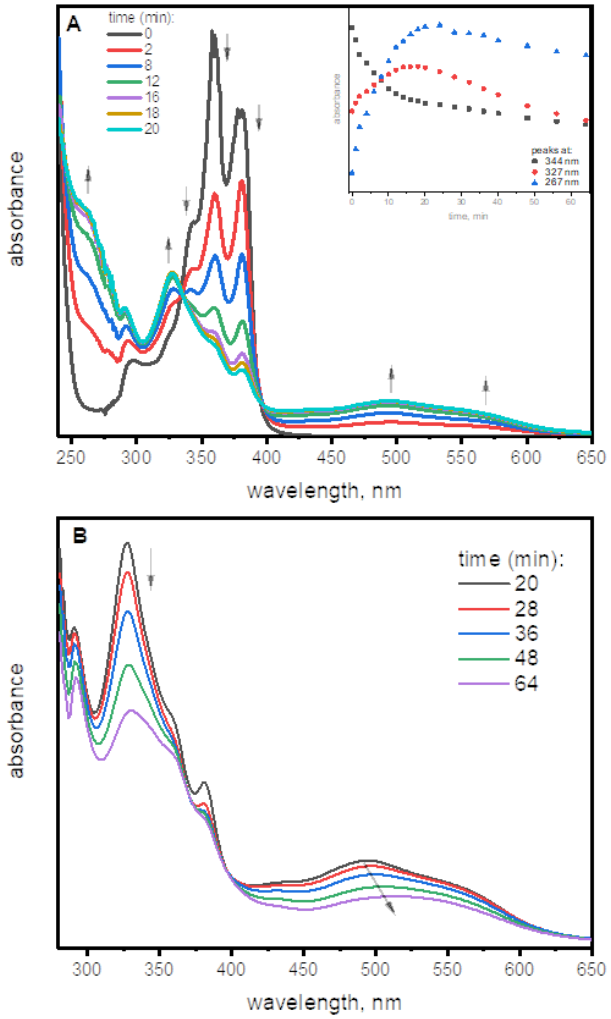

Figure 7. **DaO** [3.0×10^{-4}M] spectral changes observed in THF throughout irradiation time, λ_{exc} = 365 nm, the arrows indicate as the band peaks behave. A) spectral behaviour until 20 min; B) upon 20 min of irradiation, there was another spectral shift. The isosbestic point, at 327 nm, stands until 20 min.

These spectral changes could arise from supramolecular anion-π interactions between the bromide counter-ion and **NDI** unit via ET [9,20]. However, this explanation was ruled out because radical anions (**NDI**$^{\bullet-}$), and dianions (**NDI**$^{2-}$) were not identified by UV-vis nor EPR (not shown). Further,

reduced **NDI** moieties are extremely sensitive to air oxygen and the colour would not persist for as long as it does in the present case (samples can be stored for several days in open vials). Furthermore, the existence of an emissive state is in contrast to reduced NDIs in which fluorescence vanishes. An important issue was whether short-lived NDI radical might exist and trigger such aggregation as seen for some supramolecular systems, in which sacrificial electron donors as amines are used [21,22]. However, electrochemical runs and radical anion generators gave rise only to the expected reduced NDI species (**NDI**$^{\bullet-}$ and **NDI**$^{2-}$) and did not deliver the same spectral pattern, colour change, and air stability as seen for the photo irradiated samples (supporting information, *SI-4*).

Moreover, the existence of an absorbance isosbestic point implies at least two molecular structures related one another by either reversible structural modification or reversible aggregation [23, 24]. An interconverting system was confirmed when providing cycles under illumination and heating at each time. Light exposition at regular temperature led to (S0-S1)-absorption fading and a reddish solution while heating, and keeping at 70 °C, for 1 h brought back the structured band and partially to the initial colorless solution. Similar behaviour happened when sodium tetrafluoroborate ($NaBF_4$) was added stepwise into the reddish solution, implying that larger counter-anions impair stack formation (*supporting information, SI-5)*, Fig. 8.

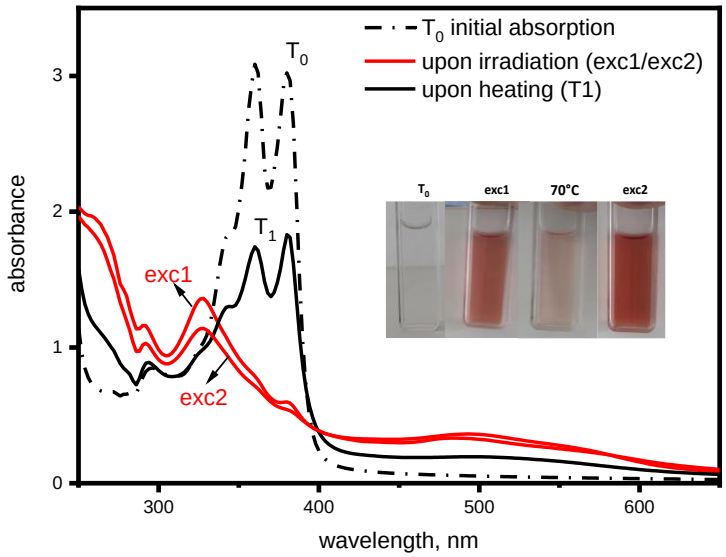

Figure 8. Light/temperature cycle showing the back-forth sensitization of the **DaO** in THF: (dashed line) initial absorption T_0; (exc1) after first irradiation for 30 min; (T1) after keeping the quartz cuvette in a bath at 70 °C for 20 min; (exc2) second irradiation for 30 min.

In order to probe the molecular basis for this **DaO** absorbance change, ^{1}H-MNR spectra were recorded over at least 3 light/temperature cycles, Fig. 9.

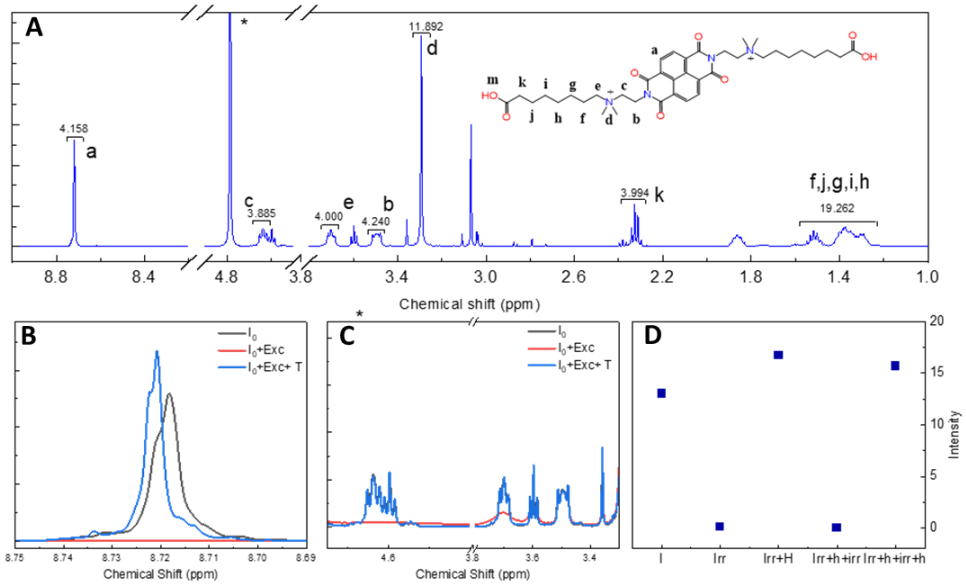

Figure 9. **A)** ^{1}H-NMR spectrum of **DaO** (D_2O 500MHz); **B)** Zoom in of the 8.72 ppm region showing the variation of the aromatic signal through the light/temperature cycle showing the back-forth sensitization of **DaO**; **C)** Zoom in the region of 4.5ppm; **D)** The intensity of the 8.72ppm signal throughout the cycle. *H_2O signal.

As shown in Fig. 9b-c, after 1h of irradiation (λ = 365 nm, 5.0 mW/cm^2), the intensity of the aryl CH hydrogen atom signal, near 8.7 ppm, decreases significantly and becomes broader. Other signals from the hydrogen atoms of the alkyl chain, also broaden and coupling becomes unresolved. The ^{1}H NMR resonances were recovered upon heating at 70°C for 100 min. This cycle was repeated, and the same tendency was observed. The intensity of the signal at 8.7 ppm was plotted (Fig. 9d) and its integral was calculated in each step of the light/temperature cycle (*supporting information, SI-5 – Table*). After the first irradiation cycle, the signal is restored. It is

narrower and its maximum intensity increases by 0.7. The integral of the signal remains almost the same, showing that the number of hydrogen atoms does not change (Fig.9b). This ^{1}H-MNR evidence points to an aggregation via π-π stacking when the sample is irradiated and that upon heating is reversed. Such an NMR spectroscopic signature toward π-π aggregation has been reported in thiophene-based conjugated polymers [24]. ^{1}H-NMR measurements at varying **DaO** concentration (Fig. SI-23) showed the same behavior for the NMR signal over the concentration range (from 6×10^{-5} to 2×10^{-3} M), implying that light can induce this peculiar aggregation even at low concentration. Overall, this represents a back-and-forth process that can be driven by distinct physical stimuli.

Given all these results we conclude that light exposure prompts a specific aggregation of the **NDI-bas** molecules leading to coupled-electronic transitions that change the dipoles of the transition's axis (L_a and L_b) [25]. Such an aggregation gives rise to a CT-electronic state as well. Moreover, the observed NDI UV-vis absorption pattern resembles that previously reported for perylene diimide within gels, owing to the twisted face-to-face packing toward gel´s fibril structure, thus, forming H-type aggregates [26]. Therefore, in the present case, photoirradiation is the driving force that causes molecules to interact one another to form H-aggregates, most likely within a twisted sandwich structure [26-29]. This arrangement may avoid electrostatic repulsion between the positively charged ammonium groups on both sides, and it allows an orthogonally close contact with increased charge transfer or excitonic coupling, Fig. 10.

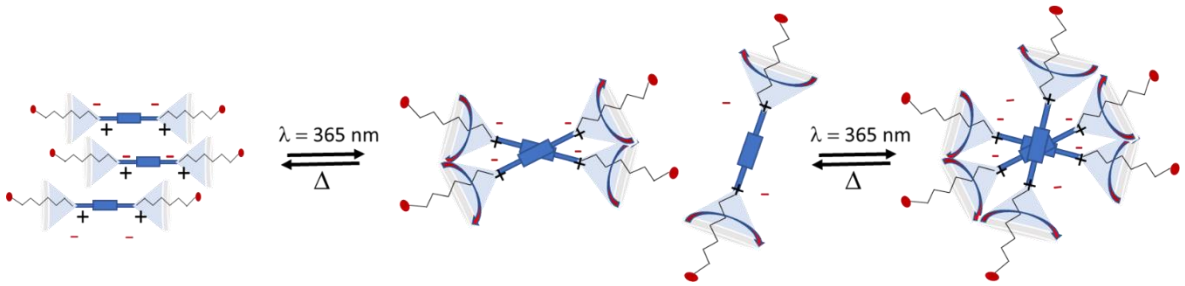

Figure 10. Model for light-induced aggregation of the **NDI-bas.**

3.3 Singlet Oxygen Photogeneration

NDI chromophores undergo excited state sensitization mechanisms that follow those verified for molecular sensitizers [30-34]. One of them (type 2) is through singlet oxygen ($^1O_2$) generated from a triplet state which occurs due to efficient singlet-triplet intersystem crossing. Other mechanisms (type 1) take place by redox reactions or by forming CT-induced self-aggregation [34]. Therefore, we evaluated the excited state properties in terms of $^1O_2$ generation as the **DaO** solution was irradiated over time, Fig. 8.

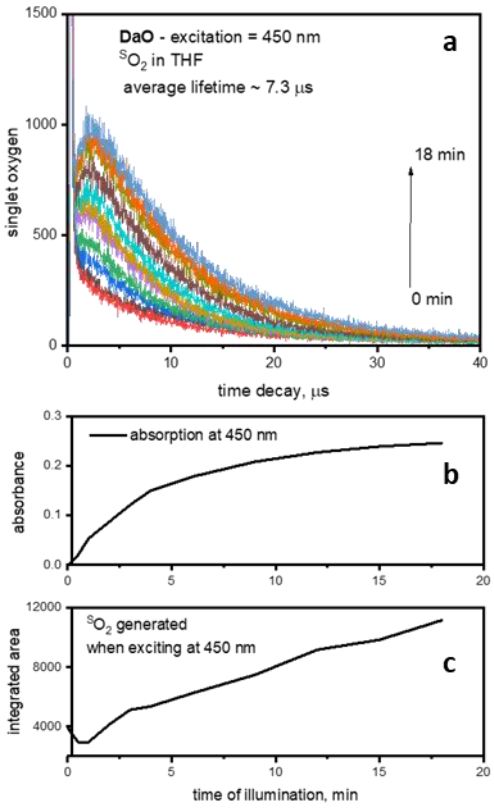

Figure 8. (a) - Singlet oxygen generation during the irradiation period; (c) the formation of $^1O_2$ (from the spectrum area) is very close to the increase (b) in absorption at 450 nm caused by **DaO** aggregation.

The amount of $^1O_2$ increased with light irradiation time along with increasing intensity of the absorption band at each of the choice excitations (*supporting information*, *SI-6*), indicating a direct relation to the formation of the aggregate form in solution. The light-induced aggregate proved to be a better sensitizer than free **DaO** in solution, pumping up the triplet state and hence enhancing the sensitization of the dissolved oxygen to the singlet form at regular temperature (supporting information *SI-7*). Such a dye-aggregation improving $^1O_2$ photogeneration is a breakthrough result since the opposite is expected regarding dye-sensitizing processes [31,32].

3.4. Time-resolved luminescence studies

At higher DaO concentrations (1×10^{-4} M) in THF at 77 K, fluorescence emission of the aggregate species predominates over monomer's (Figure 12-a and -b), and phosphorescence emission is clearly observed (Figure 12-c), whereas at room temperature, for the same concentrations, monomer fluorescence prevails (Figure 12-d and -e) and no phosphorescence could be observed. Both monomer and aggregate emission intensities are higher at 77 K than at room temperature, which could be indicative of delayed fluorescence, provided the luminescence lifetimes at these wavelengths were comparable to the phosphorescence lifetime, which is not the case (Table 1). Further studies to investigate this behaviour will be performed. It is also noteworthy that at room temperature the fluorescence band attributed to the aggregate species appears bathochromically shifted when compared to the 77 K spectra. Both fluorescence lifetimes (monomer and aggregate) increase with decreasing temperature, but remain within the same order of magnitude, certainly due to decrease of the non-radiative rate constants at 77 K. Aqueous solutions with the same concentration were also studied at room temperature, but the obtained

luminescence intensity had a very low signal-to-noise ratio, which did not allow any determinations. Like in THF, phosphorescence was also not observed.

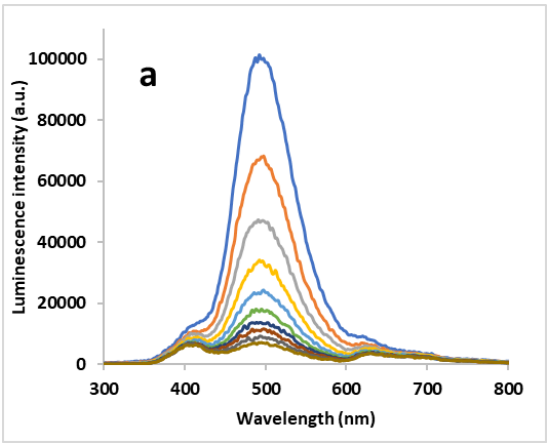

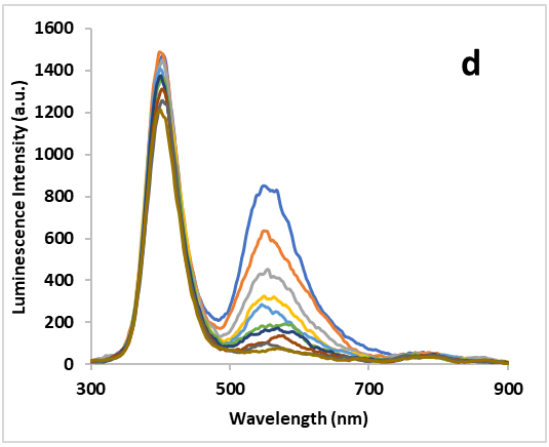

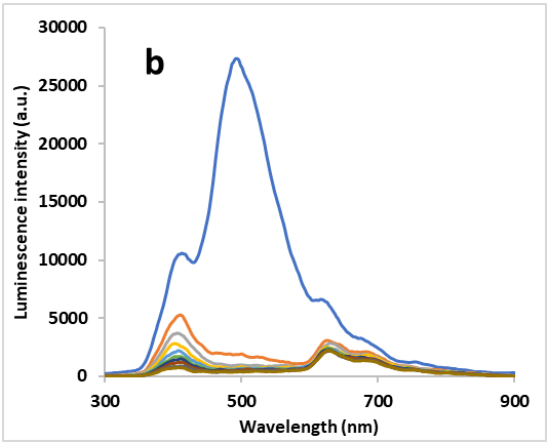

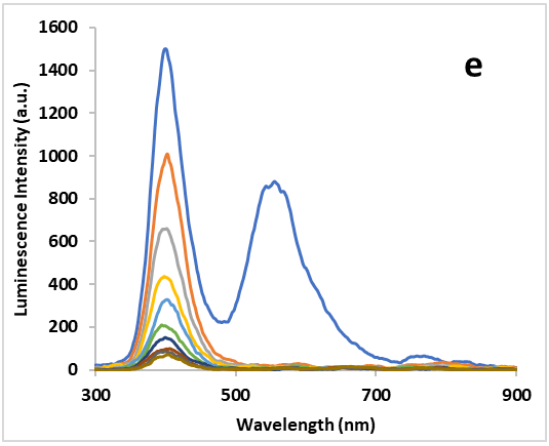

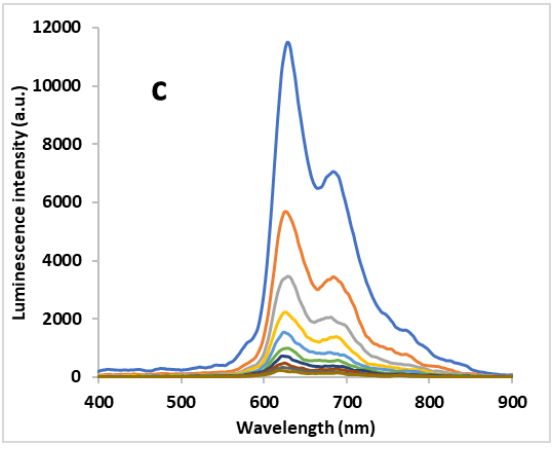

Figure 12 – Time-resolved emission spectra of DaO in THF solution (1×10^{-4} M), at 77 K (left) and at room temperature (*ca.* 293 K), Ar-purged (right). l_{exc} = 337 nm (N_2 laser). All spectra were recorded with a start delay (SD) of 0 ns (blue curve) except spectrum c, with a SD of 5 ms, and increments (step) of 10 ns (a), 100 ns (b and e), 500 ms (c), 5 ns (d), with the use of gatewidths (GW) of 10 ms (a and b), 200 ms (c) and 50 ms (d and e). The luminescence intensity decreases at each delay increment.

For more diluted **DaO** solutions (1×10^{-5} M) in THF the predominant species is the monomer, even at 77 K, as depicted in Figure 13-a and -b, and a less intense phosphorescence emission is observed when compared to the one obtained for higher DaO concentrations (Figure 12-c). Nevertheless, phosphorescence lifetime in more diluted conditions is considerably higher (a more than 40-fold enhancement), which might be indicative of less non-radiative transitions due to triplet-triplet annihilation than in the more concentrated THF solution, resulting in a longer-lived excited triplet state in the former. This observation corroborates the singlet oxygen detection experiments, in which the aggregates generated more singlet oxygen than single monomers, contrarily to what is usually expected in most sensitizers. In water (Figure 13-d and e), even at lower concentrations the predominant emission is due to the aggregate species, with a lifetime comparable to the one observed in THF. However, the fluorescence lifetime of the monomer is considerably lower than its THF solution counterpart, which points out a higher tendency to aggregate in water than in THF. This result is in agreement with what was depicted in Figure 3, where in water it is possible to observe two types of aggregate (with excitation maxima at 274 and 320 nm) whereas in THF only one aggregate species appears to be present (with excitation maximum at 326 nm). Likewise, phosphorescence lifetime in water is slightly lower than in THF

for the same concentration, which might be due to higher aggregation in water and, consequently, higher triplet-triplet annihilation rates.

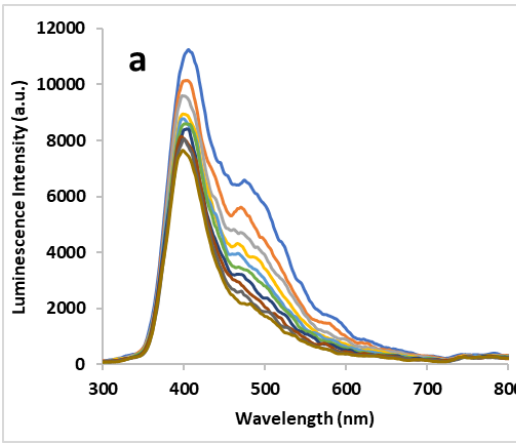

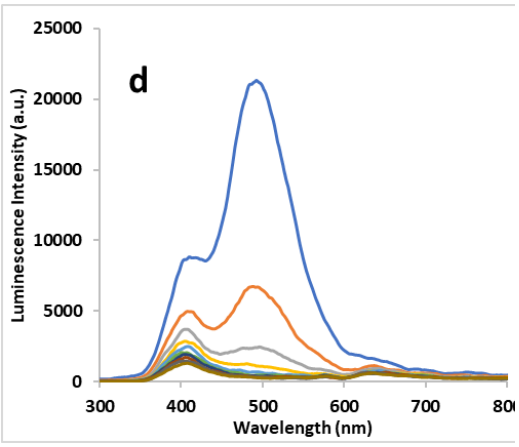

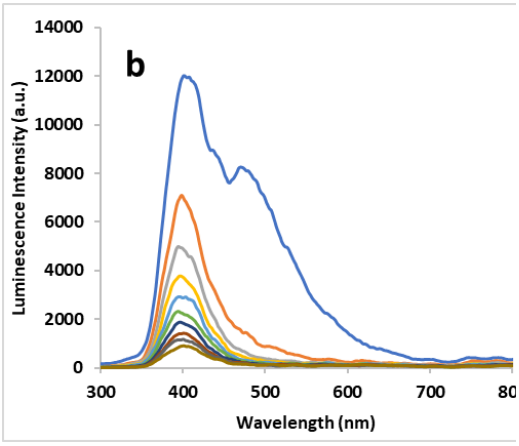

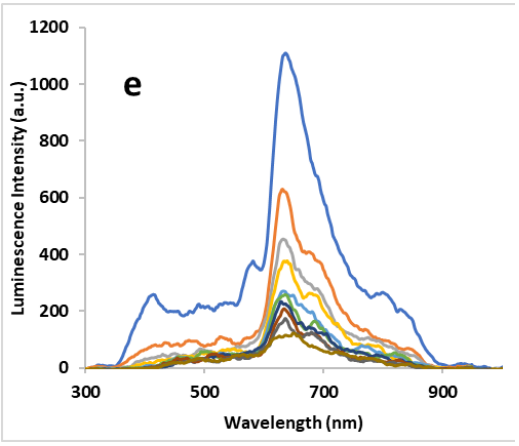

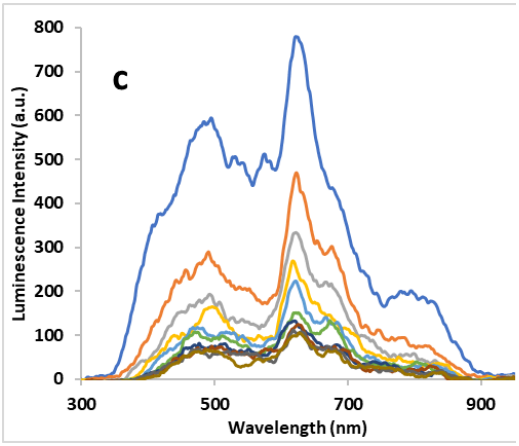

Figure 13 – Time-resolved emission spectra of DaO 1×10^{-5} M in THF (left) and H_2O (right), at 77 K. l_{exc} = 337 nm (N_2 laser). Spectra a, b and d were recorded with a start delay (SD) of 0 ns (blue curve), and spectra c and e with a SD of 5 ms, and increments (step) of 5 ns (a), 100 ns (b), 100 ms (c), 50 ns (d) and 100 ms (e), with the use of gatewidths (GW) of 50 ms (a, b and d) and 200 ms (c and e). The luminescence intensity decreases at each delay increment.

Table 1 – Photoluminescence wavelength maxima and corresponding luminescence lifetimes (τ_L)* for **DaO** in THF and water solutions, at r.t.** and 77 K.

	[DaO] = 10^{-4} M		[DaO] = 10^{-5} M			
	λ_{em}^{max} (nm)	τ_L (THF)	λ_{em}^{max} (nm)	τ_L (THF)	λ_{em}^{max} (nm)	τ_L (H_2O)
77 K	492 412 628	29 ns (agg) 260 ns (m) 10 μs (phosph)	475 401 622	43.5 ns (agg) 317 ns (m) 435 μs (phosph)	494 410 636	43 ns (agg) 144 ns (m) 377 μs (phosph)
r.t.	549 401	13 ns (agg) 216 ns (m)	-	-	-	-

* τ_L values were estimated from the half-life of photoluminescence decay obtained from the time-resolved emission spectra, thus divided by ln(2).

** r.t. = *ca.*293 K.

In conclusion, we have demonstrated that visible light can induce NDI quaternary ammonium amphiphiles to assemble when in concentrated solution. This phenomenon is a reversible process in which light promotes aggregation while increased temperature reverts the system to the initial state. The bolaamphiphiles studied **DaO**, **DaP** and **DC4** did not display a significant influence of their substituents even for the hydrogen bonding COOH group. UV-vis and NMR spectroscopy confirmed the reversibility of the aggregation and imply that it arises from π-stacking that is likely to be connected to an H-aggregate. Such aggregates acquire different photochemical properties, particularly the generation of singlet oxygen which is unprecedented from the point of view of sensitizer properties. We envision this system has the possibility of being

used as an on/off switch to conveniently and controllably generate singlet $^1O_2$, a strong oxidant, which can be used in chemical reactions and oxide formation. So far, this represents the first description of light incidence prompting aggregation of NDI amphiphiles. These findings highlight an important lesson, that at high concentration, illumination may result in persistent self-assembly in a way that it induces NDI-NDI interactions and photophysical changes that might be easily mistaken for intermolecular donor-acceptor CT-events usually observed in supramolecular systems.

Acknowledgement

The São Paulo Research Foundation - FAPESP for grants 2021/01509-0, 2022/06346-5 (Eduardo Rezende Triboni), 2022/02711-0 (Rafael Gagliardi Antoneli), 2019/27157-3 (Thaisa Brandão Ferreira de Moraes). NAP-Phototech, USP-SP, for singlet oxygen analysis. SiSNano-USP, PRP-USP PIPAE num 2021.1.10424.1.9, and CNPq (Brazilian National Research Council) grant 315064/2021-8 (Gregóire J-.F. Demets). Institute for Bioengineering and Biosciences acknowledges the financial support of FCT (UIDB/04565/2020 and UIDP/04565/2020). The Associate Laboratory Institute for Health and Bioeconomy (i4HB) acknowledges the financial support of FCT (LA/P/0140/2020). JWS thanks the Engineering and Physical Sciences Research Council for support (EP/S035877/1). We would like to thank Professor Mario José Politi (IQ-USP) for the helpful discussion on naphtalenediimide photophysics.

References

1. Maniam, S., Higginbotham, H. F., Bell, T. D., & Langford, S. J. (2019). Harnessing brightness in naphthalene diimides. *Chemistry–A European Journal*, *25*(29), 7044-7057.

2. Bhosale, S. V., Jani, C. H., Langford, S. J. (2008). Chemistry of naphthalene diimides. *Chemical Society Reviews*, *37*(2), 331-342.

3. Bhosale, S. V., Al Kobaisi, M., Jadhav, R. W., Morajkar, P. P., Jones, L. A., & George, S. (2021). Naphthalene diimides: perspectives and promise. *Chemical Society Reviews*.

4. Zhou, Q., Chen, T., Zhang, J., Wan, L., Xie, P., Han, C. CZhang, R. (2008). Hierarchical self-assembly of p-terphenyl derivative with dumbbell-like amphiphilic and rod-coil characteristics. *Tetrahedron Letters*, *49*(38), 5522-5526.

5. Pantos, G. D. (Ed.). (2017). *Naphthalenediimide and its Congeners: From molecules to materials*. Royal Society of Chemistry.

6. Rajdev, P., Chakraborty, S., Schmutz, M., Mesini, P., & Ghosh, S. (2017). Supramolecularly Engineered π-Amphiphile. *Langmuir*, *33*(19), 4789-4795.

7. Tam, T. L. D., & Xu, J. W. (2019). The role of fluoride in anion–π interaction with naphthalene diimide. *Chemical Communications*, *55*(44), 6225-6228.

8. Schottel, B. L., Chifotides, H. T., Dunbar, K. R. (2008). Anion-π interactions. *Chemical Society Reviews*, *37*(1), 68-83.

9. Guha, S., Goodson, F. S., Corson, L. J., Saha, S. (2012). Boundaries of anion/naphthalenediimide interactions: from anion− π interactions to anion-induced charge-transfer and electron-transfer phenomena. *Journal of the American Chemical Society*, *134*(33), 13679-13691.

10. Das, A., & Ghosh, S. (2016). H-bonding directed programmed supramolecular assembly of naphthalene-diimide (NDI) derivatives. *Chemical Communications*, *52*(42), 6860-6872.

11. Molla, M. R., Gehrig, D., Roy, L., Kamm, V., Paul, A., Laquai, F., & Ghosh, S. (2014). Self-assembly of carboxylic acid appended naphthalene diimide derivatives with tunable luminescent color and electrical conductivity. *Chemistry–A European Journal*, *20*(3), 760-771.

12. Rajdev, P., Molla, M. R., & Ghosh, S. (2014). Understanding the role of H-bonding in aqueous self-assembly of two naphthalene diimide (NDI)-conjugated amphiphiles. *Langmuir*, *30*(8), 1969-1976.

13. Castaldelli, E., Triboni, E. R., Demets, G. J. F. (2011). Self-assembled naphthalenediimide derivative films for light-assisted electrochemical reduction of oxygen. *Chemical Communications*, *47*(19), 5581-5583.

14. Moraes, T. B., Schimidt, M. F., Bacani, R., Weber, G., Politi, M. J., Castanheira, B.,Triboni, E. R. (2018). Polysilsesquioxane naphthalenediimide thermo and photochromic gels. *Journal of Luminescence*, *204*, 685-691.

15. Barros, T. C., Brochsztain, S., Toscano, V. G., Berci Filho, P., Politi, M. J. (1997). Photophysical characterization of a 1, 4, 5, 8-naphthalenediimide derivative. *Journal of Photochemistry and Photobiology A: Chemistry*, *111*(1-3), 97-104.

16. Wang, W., Han, J. J., Wang, L. Q., Li, L. S., Shaw, W. J., & Li, A. D. (2003). Dynamic π− π stacked molecular assemblies emit from green to red colors. *NanoLetters*, *3*(4), 455-458.

17. Zhao, Z., WY Lam, J., & Zhong Tang, B. (2010). Aggregation-induced emission of tetraarylethene luminogens. *Current Organic Chemistry*, *14*(18), 2109-2132.

18. Ponnuswamy, N., Pantos, G. D., Smulders, M. M., & Sanders, J. K. (2012). Thermodynamics of supramolecular naphthalenediimide nanotube formation: the influence of solvents, side chains, and guest templates. *Journal of the American Chemical Society*, *134*(1), 566-573.

19. Gonzalez, L., Liu, C., Dietrich, B., Su, H., Sproules, S., Cui, H., Draper, E. R. (2018). Transparent-to-dark photo-and electrochromic gels. *Communications Chemistry*, *1*(1), 1-8.

20. Guha, S., & Saha, S. (2010). Fluoride ion sensing by an anion− π interaction. *Journal of the American Chemical Society*, *132*(50), 17674-17677.

21. Ellis, T. K., Galerne, M., Armao IV, J. J., Osypenko, A., Martel, D., Maaloum, M., Giuseppone, N. (2018). Supramolecular electropolymerization. *Angewandte Chemie*, *130*(48), 15975-15979.

22. Paulino, V., Mukhopadhyay, A., Tsironi, I., Liu, K., Husainy, D., Liu, C, Olivier, J. H. (2021). Molecular Engineering of Water-Soluble Oligomers to Elucidate Radical π–Anion Interactions in n-Doped Nanoscale Objects. *The Journal of Physical Chemistry C*, *125*(19), 10526-10538.

23. Bukleski, M., Dimitrovska-Lazova, S., Makrievski, V., & Aleksovska, S. (2020). A simple approach for determination of the phase transition temperature using infrared temperature-induced isosbestic points. *Spectrochimica Acta Part A: Molecular and Biomolecular Spectroscopy*, *231*, 118118.

24. Nowicka-Jankowska, T. (1971). Some properties of isosbestic points. *Journal of Inorganic and Nuclear Chemistry*, *33*(7), 2043-2050.

25. Gawroński, J., Gawrońska, K., Skowronek, P., Holmen, A. (1999). 1, 8-Naphthalimides as stereochemical probes for chiral amines: A study of electronic transitions and exciton coupling. The Journal of Organic Chemistry, 64(1), 234-241.

26. Würthner, F., Bauer, C., Stepanenko, V., & Yagai, S. (2008). A black perylene bisimide super gelator with an unexpected J-type absorption band. *Advanced Materials*, *20*(9), 1695-1698.

27. Shigemitsu, H., Ohkubo, K., Sato, K., Bunno, A., Mori, T., Osakada, Y., Kida, T. (2022). Fluorescein-Based Type I Supramolecular Photosensitizer via Induction of Charge Separation by Self-Assembly. JACS Au 2022, 2(6), 1472–1478.

28. Barros, T. C., Brochsztain, S., Toscano, V. G., Berci Filho, P., & Politi, M. J. (1997). Photophysical characterization of a 1, 4, 5, 8-naphthalenediimide derivative. *Journal of Photochemistry and Photobiology A: Chemistry*, *111*(1-3), 97-104.

29. Dixon, D. W., Thornton, N. B., Steullet, V., & Netzel, T. (1999). Effect of DNA scaffolding on intramolecular electron transfer quenching of a photoexcited ruthenium (II) polypyridine naphthalene diimide. *Inorganic chemistry*

30. Parenti, F., Tassinari, F., Libertini, E., Lanzi, M., Mucci, A. (2017). π-Stacking signature in NMR solution spectra of thiophene-based conjugated polymers. *ACS omega*, *2*(9), 5775-5784.

31. Junqueira, H. C., Severino, D., Dias, L. G., Gugliotti, M. S., & Baptista, M. S. (2002). Modulation of methylene blue photochemical properties based on adsorption at aqueous micelle interfaces. *Physical Chemistry Chemical Physics*, *4*(11), 2320-2328.

32. Shigemitsu, H., Ohkubo, K., Sato, K., Bunno, A., Mori, T., Osakada, Y., Kida, T. (2022). Fluorescein-Based Type I Supramolecular Photosensitizer via Induction of Charge Separation by Self-Assembly. JACS Au 2022, 2(6), 1472–1478.

33. Barros, T. C., Brochsztain, S., Toscano, V. G., Berci Filho, P., & Politi, M. J. (1997). Photophysical characterization of a 1, 4, 5, 8-naphthalenediimide derivative. *Journal of Photochemistry and Photobiology A: Chemistry*, *111*(1-3), 97-104.

34. Dixon, D. W., Thornton, N. B., Steullet, V., & Netzel, T. (1999). Effect of DNA scaffolding on intramolecular electron transfer quenching of a photoexcited ruthenium (II) polypyridine naphthalene diimide. *Inorganic chemistry*